# Effect of TiO$_2$ on the Viscosity and Slag Structure in Blast Furnace Type Slags

Hyunsik Park, Jun-Young Park, Gi Hyun Kim, and Il Sohn*

TiO$_2$ additions up to 10 mass% behaved as a basic oxide and lowered the viscosity in the CaO–SiO$_2$–17 mass% Al$_2$O$_3$–10 mass% MgO-based slags by depolymerizing the silicate network structure. Raman spectroscopy revealed the sum of NBO/Si 1 and 3 decreased while the sum of NBO/Si 2 and 4 increased with TiO$_2$ content. Unlike the silicate structures, the aluminate structures seems to be relatively unaffected by TiO$_2$ additions according to the FTIR results. 5 mass% TiO$_2$ significantly decreased the viscosity compared to the TiO$_2$ free slags, but beyond 5 mass% TiO$_2$ meaningful changes in the viscosity was not observed. From the comparison of the viscosity at constant TiO$_2$ of 5 and 10 mass% and varying CaO/SiO$_2$ ratio, increasing the CaO/SiO$_2$ ratio was more effective in decreasing the viscosity than TiO$_2$ additions.

## 1. Introduction

Cost issues related to integrated steel mill operations and unavailability of high grade raw materials with high concentrations of iron has sparked interest in the use of other potential sources of iron bearing materials once regarded as uneconomical for the present day integrated steel mill operations. In particular, iron ores consisting of significant TiO$_2$ such as ilmenite is comparatively abundant in Australia and other parts of the world. These ores due to the high TiO$_2$ content may result in significant issues such as lower reduction degree of the ore,[1–4] variations in the liquidus temperature of the slag,[5–7] reduced refining capacity of the slag,[8–10] and slag viscosity deviations from optimum processing conditions.[11–15]

However, potential benefits of TiO$_2$ in the blast furnace slags have also been realized from work done by Morizane et al.[9] and others.[15–18] By forming a protective layer of titanium carbo-nitride on the refractory brick, the premature failure and erosion of the hearth was found to be inhibited. Thus, both the thermophysical and chemical properties of the slag can change with TiO$_2$ additions and a fundamental understanding on these topics, in particular the effect of viscosity, is essential to maintain and optimize the overall efficiency of the blast furnace operations.

Handfield and Charette[12] showed small TiO$_2$ additions can decrease the slag viscosity, but large TiO$_2$ additions had the opposite effect. Ohno and Ross[13] described TiO$_2$ additions to increase slag viscosity in the CaO–SiO$_2$–Al$_2$O$_3$–TiO$_2$ slags under reducing conditions. Work done by Shankar et al.[19] showed the effect of TiO$_2$ in the CaO–SiO$_2$–MgO–Al$_2$O$_3$ slag system under Ar, where TiO$_2$ up to 2 mass% decreased the viscosity at various fixed extended Vee ratio [(CaO + MgO)/(SiO$_2$ + Al$_2$O$_3$)] between 0.46 and 0.83. Saito et al.[14] also studied the effect of TiO$_2$ in the CaO–SiO$_2$–MgO–Al$_2$O$_3$ slag system at 10 and 20 mass% TiO$_2$ content. TiO$_2$ lowered the viscosity of the slag and the corresponding activation energy of viscous flow decreased with TiO$_2$ content. Thus, slag viscosity can be affected by the amount of TiO$_2$ additions. However, to the knowledge of the authors, the viscosity data between 0 and 10 mass% TiO$_2$ is not well defined for blast furnace type slags and its correlation with the slag structure has yet to be fully understood.

Therefore, understanding and controlling the effects of TiO$_2$ on the viscosity of blast furnace type slags, when raw materials' containing significant amounts of TiO$_2$ such as ilmenite is utilized, would be essential in maintaining stable blast furnace operations. In this work, the influence of TiO$_2$ on the viscous behavior of calcium-silicate based slags with 17 mass% Al$_2$O$_3$ and 10 mass% MgO based slags have been studied using a rotating viscometer. To directly correlate the relationship between slag structure and viscosity, flux samples from the fully liquid region at 1773 K were quenched and analyzed using Fourier transform infra-red (FTIR) and Raman spectroscopy.

[*] J.-Y. Park, G. Hyun Kim, Prof. I. Sohn
  Materials Science and Engineering, Yonsei University
  Seoul 120-749, Korea
  Email: ilsohn@yonsei.ac.kr
  H. Park
  Department of Materials Science and Engineering, Formerly Research
  Assistant at the Research Institute of Iron and Steel Technology
  Yonsei University, New South Wales, Australia

## 2. Experimental Methods

### 2.1. Materials

Slags were prepared using reagent grade chemicals of CaO, $SiO_2$, MgO, $Al_2O_3$, and $TiO_2$. Using a Pt-10 mass% Rh crucible, slags were premelted under $0.4\,L\,min^{-1}$ of Ar to obtain a homogeneous mixture of $CaO–SiO_2–17$ mass% $Al_2O_3–10$ mass% MgO. After 3 h, the homogenized samples were quenched and crushed for the primary experiments. Chemical composition of the post-experimental slags was analyzed using X-ray fluorescence (XRF) spectroscopy (S4 Explorer; Bruker AXS GmbH, Karlsruhe, Germany) and no apparent change was observed. Thus, the initial weighed mixture was taken as the slag composition. The experimental chemical composition is given in **Table 1**.

### 2.2. Apparatus and Procedure

The viscosity was measured using a rotating spindle connected to a calibrated Brookfield digital rheometer (LVDV-II+; Brookfield Engineering Laboratories, Middleboro, MA). The details of the experimental apparatus have been given elsewhere,[20,21] but a schematic diagram is shown in **Figure 1**.

Samples weighing 120 g were prepared according to Table 1 and placed in a Pt-10 mass% Rh crucible (H: 60 mm, ID: 40 mm). Furnace temperature was calibrated using a reference B-type thermocouple and controlled within $\pm 3\,K$ using a PID controller. Slag samples were heated to 1773 K and sufficiently held for more than an hour in an Ar gas atmosphere to achieve thermal equilibrium. Measurements were taken at each target temperature during a $5\,^{\circ}C\,min^{-1}$ cooling cycle after 30 min of

soaking and in the fully liquid region of the slag system well above the break temperature ($T_{Br}$) of each slag composition. The break temperature has been described in detail by Kim and Sohn[21] and Sridhar et al.[22] Viscosity measurements taken at temperatures higher than the break temperature are assumed to be in the fully liquid region of the slag system, of which the present experimental measurements have been done. The break temperature can easily be identified using the example given in **Figure 2** for the $CaO–SiO_2–17$ mass% $Al_2O_3–10$ mass% $MgO–5$ mass% $TiO_2$ slag at constant $CaO/SiO_2$ of 1.2. The natural logarithm of viscosity ($\ln\,\eta$) as a function of reciprocal temperature ($1/T$) shows a significant increase below temperatures of 1598 K, which is the starting temperature for the formation of large solid precipitates. Viscosity measurements were also taken during a heating cycle of $5\,^{\circ}C\,min^{-1}$ and 30 min of soaking time, but no appreciable difference was found during measurements in the fully liquid region of the slag system and thus subsequent viscosity measurements were done during the cooling cycle.

After completing the viscosity measurements, slag samples were reheated to 1773 K and quenched on a water-cooled copper plate to confirm the slag structure using FTIR (Spectrum 100 Optica; Perkin-Elmer, USA) and Raman spectroscopy (PD-RSM300; Photon Design, Japan) with a 514 nm laser. Non-parametric baseline fitting routine was used and the deconvolution was performed by Peak Fit V4 (Systat Software Inc, USA). Sample removal from the hot zone of the furnace and pouring onto the copper plate took less than 10 s. Preliminary X-ray diffraction (XRD) analysis of the transparent samples resulted in negligible characteristic diffraction peaks indicating the sample to be amorphous and representative of the slags molten structural state. Wang and Cramb[23] were also able

| No. | Composition (mass%) | | | | | C/S | Viscosity (Pa s$^{-1}$) | | | | | | | |
|---|---|---|---|---|---|---|---|---|---|---|---|---|---|---|
| | CaO | SiO$_2$ | Al$_2$O$_3$ | MgO | TiO$_2$ | | 1325 (°C) | 1350 (°C) | 1375 (°C) | 1400[a] (°C) | 1425 (°C) | 1450[a] (°C) | 1475 (°C) | 1500[a] (°C) |
| 1 | 33.2 | 39.8 | 17 | 10 | 0 | 0.8 | – | – | 0.98 | 0.76 | 0.63 | 0.51 | 0.43 | 0.34 |
| 2 | 30.9 | 37.1 | 17 | 10 | 5 | 0.8 | – | 0.92 | 0.73 | 0.56 | 0.45 | 0.37 | 0.30 | 0.25 |
| 3 | 28.6 | 34.4 | 17 | 10 | 10 | 0.8 | 1.01 | 0.76 | 0.61 | 0.48 | 0.41 | 0.33 | 0.27 | 0.24 |
| 4 | 36.5 | 36.5 | 17 | 10 | 0 | 1.0 | – | – | – | 0.69 | 0.54 | 0.43 | 0.35 | 0.28 |
| 5 | 34.0 | 34.0 | 17 | 10 | 5 | 1.0 | – | – | – | 0.52 | 0.39 | 0.32 | 0.28 | 0.23 |
| 6 | 31.5 | 31.5 | 17 | 10 | 10 | 1.0 | – | – | – | 0.48 | 0.39 | 0.28 | 0.24 | 0.21 |
| 7 | 40.6 | 32.4 | 17 | 10 | 0 | 1.2 | | | | 0.56 | 0.42 | 0.33 | 0.27 | 0.22 |
| 8 | 37.8 | 30.2 | 17 | 10 | 5 | 1.2 | 1.04 | 0.79 | 0.60 | 0.46 | 0.35 | 0.28 | 0.22 | 0.17 |
| 9 | | | 17 | 10 | 10 | 1.2 | 1.01 | 0.75 | 0.52 | 0.42 | 0.31 | 0.24 | 0.19 | 0.14 |

[a]Data provided by the authors in a previous publication for the calculation of the activation energy.[24]

**Table 1.** Measured viscosities of $CaO–SiO_2–Al_2O_3–MgO–TiO_2$ slags.
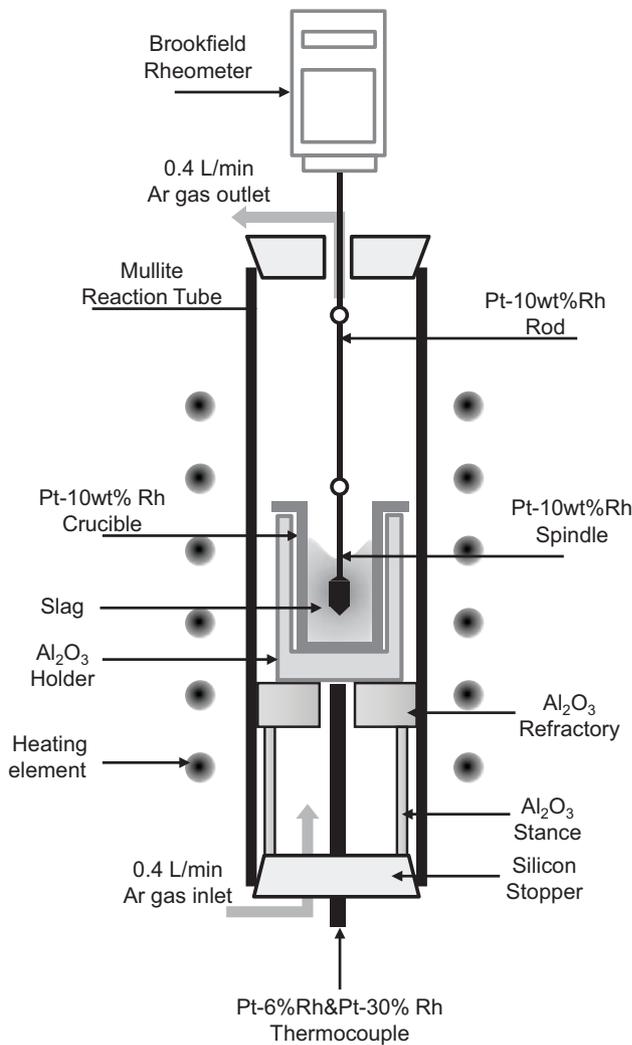
**Figure 1.** Experimental apparatus for the slag viscosity measurements.
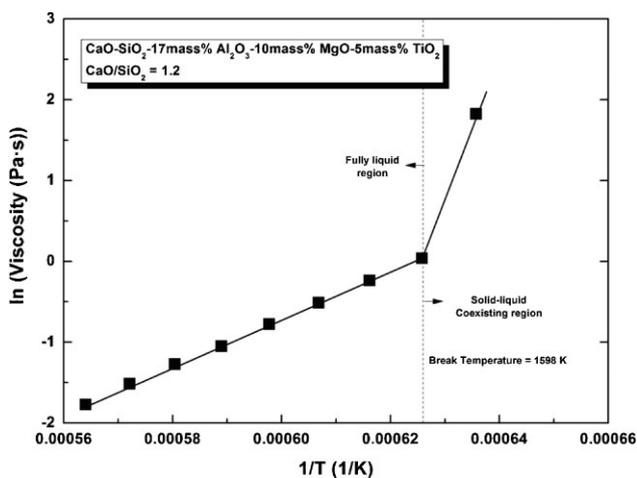
to obtain a completely amorphous sample on a water-cooled copper plate, which was similar to the quenching method applied to the present study.

## 3. Results and Discussion

### 3.1. Effect of TiO₂ on the Viscosity

**Figure 3** shows the viscosity of the CaO–SiO₂–17 mass% Al₂O₃–10 mass% MgO-based slag with TiO₂ additions and a constant CaO/SiO₂ of 1.0 at various temperatures from 1673 to 1773 K. Similar to previously published work by the authors[24] at constant CaO/SiO₂ of 0.8, TiO₂ additions at 5 and 10 mass% decreased the viscosity at the temperature range of interest. The initial addition of TiO₂ of 5 mass% lowers the viscosity of the slag and the effect of the initial TiO₂ additions of 5 mass% seems to be more pronounced at lower temperatures and is evident from the linear slope between 0 and 5 mass% TiO₂. Further additions of TiO₂ above 5 mass% has only a slight or negligible effect in lowering the viscosity. According to work done by others,[13,25] TiO₂ was suggested to be a weak acidic oxide in a basic slag system, which would increase the network structure of the slag by polymerizing the molten slag, and thus increasing the viscosity. However, the present results seem to show that TiO₂ additions decrease the viscosity, which contradicts the behavior of a network forming acidic oxide. Thus, the decrease in the viscosity with TiO₂ additions seems to suggest that TiO₂ behaves as a basic oxide contrary to some results[13,25] and subsequently depolymerizes the slags network structure.

Similar trends were also observed in **Figure 4** for the CaO–SiO₂–17 mass% Al₂O₃–10 mass% MgO–TiO₂ slag system at a fixed CaO/SiO₂ of 1.2. TiO₂ additions decreased



**Figure 2.** Break temperature ($T_{Br}$) for the CaO–SiO₂–17 mass% Al₂O₃–10 mass% MgO–5 mass% TiO₂ slag system at a fixed C/S ratio of 1.2. Break temperature was 1598 K (1325 °C).
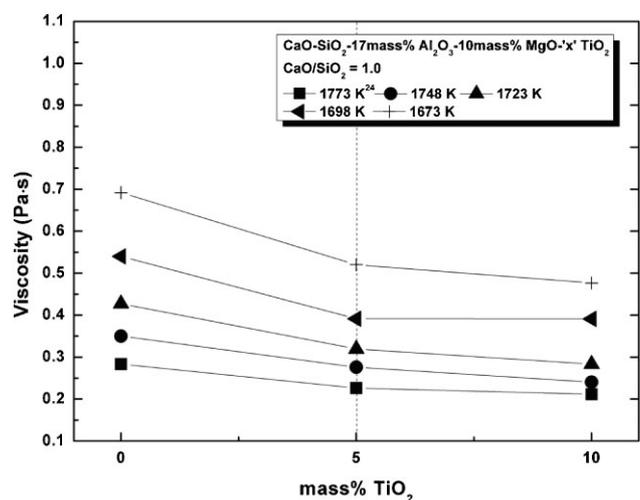


**Figure 3.** Effect of TiO₂ additions on the viscosity in the CaO–SiO₂–17 mass% Al₂O₃–10 mass% MgO–$x$TiO₂ slag system at constant CaO/SiO₂ of 1.0 and various temperatures.
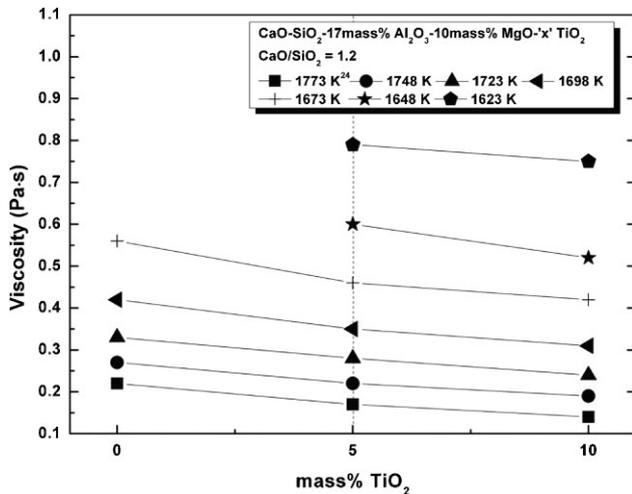
**Figure 4.** Effect of $TiO_2$ additions on the viscosity in the CaO–$SiO_2$–17 mass% $Al_2O_3$–10 mass% MgO–$x$TiO$_2$ slag system at constant CaO/$SiO_2$ of 1.2 and various temperatures.

the viscosity, but the initial effect of 5 mass% $TiO_2$ at higher basicities is not as pronounced as the slag at CaO/$SiO_2$ of 1.0. This dampened effect of $TiO_2$ at higher CaO/$SiO_2$ of 1.2 is likely due to the additional depolymerization caused by higher concentrations of CaO compared to the CaO/$SiO_2$ of 1.0.

TiO$_2$ additions at constant temperatures of 1698 and 1773 K at CaO/$SiO_2$ ratio of 0.8 and 1.2 decreases the viscosity as observed in **Figure 5**. Similar to the results observed in Figure 3, comparison of the initial slope of 5 mass% $TiO_2$ additions and the slope between 5 and 10 mass% $TiO_2$ additions suggest the effect of $TiO_2$ additions becomes less pronounced after the slag becomes significantly depolymerized.
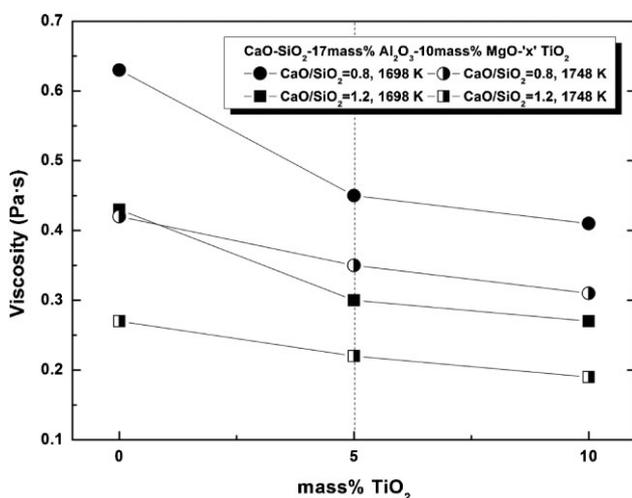
## 3.2. Effect of CaO/$SiO_2$ on the Viscosity

The effect of CaO/$SiO_2$ at $TiO_2$ of 5 and 10 mass% at 1698 and 1748 K is shown in **Figure 6**. Regardless of the $TiO_2$ content and temperature, increased CaO/$SiO_2$ lowered the slag viscosity. Higher CaO/$SiO_2$ ratio is likely to have depolymerized the slags silicate network structure and lowered the viscosity by providing additional free oxygen ions ($O^{2-}$). $TiO_2$ additions of 5 and 10 mass% had comparatively less effect on lowering the viscosity than increasing the CaO/$SiO_2$ ratio. Considering the highly basic nature of CaO compared to $TiO_2$ as suggested by Banya[26] using the ion–oxygen attraction suggested by Ward,[27] an increase in the CaO content should be more effective in depolymerizing the slag structure and lowering the viscosity compared to $TiO_2$. Shankar et al.[19] has also showed similar trends with higher CaO/$SiO_2$ in blast furnace type slags with lower MgO.

## 3.3. Effect of $TiO_2$ on the Slag Structure Using FTIR and Raman Spectroscopy

The FTIR results at constant CaO/$SiO_2$ of 0.8 and 1.2 is shown in **Figure 7**a,b, respectively, which further support the role of $TiO_2$ as a basic oxide and a network modifier. There are several characteristics of the FTIR results in $TiO_2$-containing CaO–$SiO_2$–17 mass% $Al_2O_3$–10 mass% MgO quinternary slag systems. FTIR spectra of silicate slags are typically focused within the wavenumber region between 1200 and 400 $cm^{-1}$.[20,28,29] This region represents the symmetric stretching vibration bands of the [$SiO_4$]-tetrahedra, the asymmetric stretching vibrations of the [$AlO_4$]-tetrahedra, and the symmetric Si–O bending vibration bands, etc.



**Figure 5.** Effect of $TiO_2$ additions on the viscosity in the CaO–$SiO_2$–17 mass% $Al_2O_3$–10 mass% MgO–$x$TiO$_2$ slag system at various CaO/$SiO_2$ ratio.
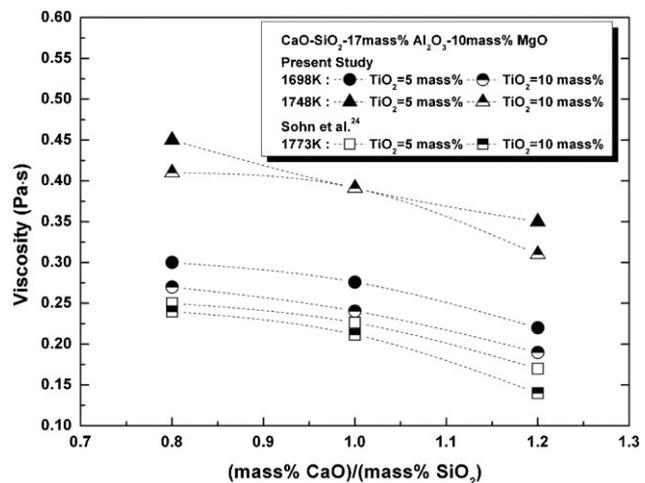


**Figure 6.** Effect of CaO/$SiO_2$ on the viscosity of the CaO–$SiO_2$–17 mass% $Al_2O_3$–10 mass% MgO–$TiO_2$ slags at 1773 K.
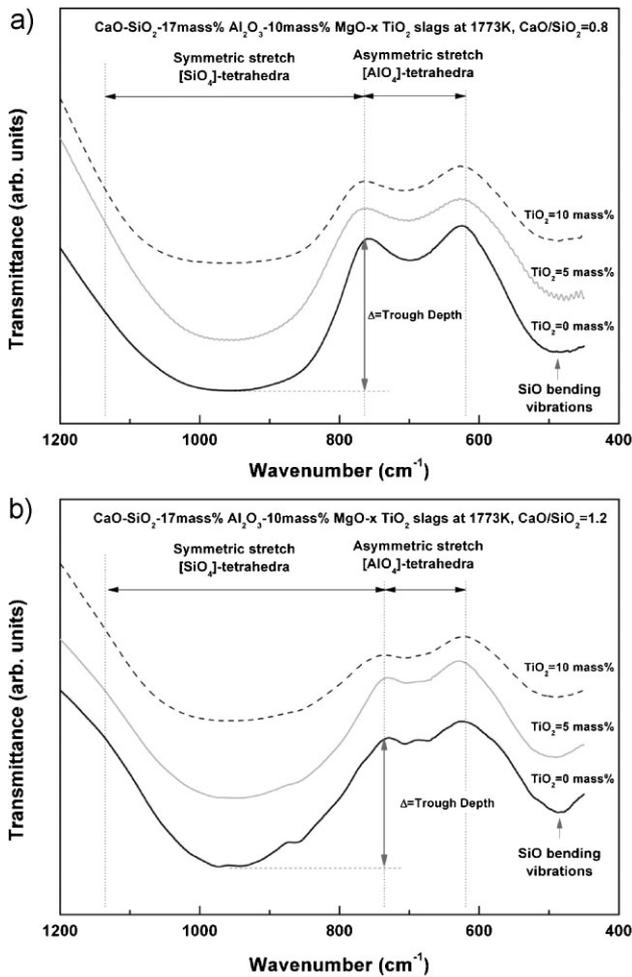
**Figure 7.** FTIR result of as-quenched samples from 1773 K with varying $TiO_2$ concentration in $CaO–SiO_2–17\,mass\%\ Al_2O_3–10\,mass\%\ MgO–TiO_2$ slags at $CaO/SiO_2$ of a) 0.8 and b) 1.2.



**Figure 8.** Deconvoluted Raman spectra of as-quenched samples from 1773 K with varying $TiO_2$ concentration in $CaO–SiO_2–17\,mass\%\ Al_2O_3–10\,mass\%\ MgO–TiO_2$ slags at $CaO/SiO_2 = 0.8$.

The vibration band between the wavenumbers of 1200 and $800\,cm^{-1}$ is the $[SiO_4]$-tetrahedra symmetric stretching vibration band, which are well known to be the convoluted band of the NBO/Si transmission troughs from NBO/Si of 1–4. This characteristic stretching vibration band for the large silicate network structures becomes less pronounced and the depth of the convoluted band becomes shallower with $TiO_2$ additions. NBO/Si is the non-bridged oxygen per unit silicon atom, where lower NBO/Si pertains to the more polymerized slag structure. According to Mysen et al.,[30] NBO/Si assigned values from 1 to 4 are structurally defined as sheets ($1100–1050\,cm^{-1}$), chains ($980–950\,cm^{-1}$), dimers ($920–900\,cm^{-1}$), and monomers ($880–850\,cm^{-1}$), respectively. This decrease in the depth of the transmission trough indicates a depolymerization of the slag structure as suggested in previously published literature.[20,21]

No significant differences could be ascertained from the asymmetric stretching vibration bands for $[AlO_4]$-tetrahedra. However, the depth of the symmetric Si–O bending vibration band from 600 to $520\,cm^{-1}$ decreased with higher $TiO_2$ as shown in Figure 7a,b. Since the Si–O bending vibrations typically becomes more pronounced with a higher degree of polymerization, the decreased depth of the FTIR transmittance from 600 to $520\,cm^{-1}$ further suggests that the slags are becoming depolymerized.[31,32] Therefore, the FTIR analysis seems to suggest that $TiO_2$ depolymerizes the slag by modifying the silicate structure

of the slags, but has little or no effect on the aluminate structure of the slag for the present slag compositions.

The as-quenched slag structure was also studied using Raman spectroscopy. **Figure 8** shows the raw Raman spectra for the CaO–SiO$_2$–17 mass% Al$_2$O$_3$–10 mass% MgO-based slags containing 0–10 mass% TiO$_2$. Deconvolution of the Raman spectra qualitatively showed several [SiO$_4$]-tetrahedra peaks with symmetric stretching vibrations pertaining to NBO/Si of 1,2,3,4 and asymmetric stretching vibrations of NBO/Si 0 near 1040 and 1170 cm$^{-1}$. Ti–O–Ti stretching vibrations are observed near 830 cm$^{-1}$.[33] Integration of the deconvoluted spectra provides a semi-quantitative value of the various silicate species as a function of TiO$_2$ content, which is plotted in **Figure 9**a,b. According to the results of the deconvoluted Raman spectra, the sum of the NBO/Si of 1 and 3 decrease and the sum of the NBO/Si of 2 and 4 increase with TiO$_2$ additions.

The decrease in the sum of NBO/Si of 1 and 3 is an indication of depolymerization occurring within the silicate structure. The depolymerization mechanism can

**Figure 10.** Temperature dependence for the CaO–SiO$_2$–17 mass% Al$_2$O$_3$–10 mass% MgO–$x$TiO$_2$ slag system at CaO/SiO$_2$ of 1.2 and various TiO$_2$ content.

be speculated to occur by reaction[1] proposed by Mysen et al.[30]

$$Q^1 + Q^3 \leftrightarrow 2Q^2 \tag{1}$$

Furthermore, the increment in the fraction of [SiO$_4$]-tetrahedra species (NBO/Si = 1,2,3,4) was significant with an initial 5 mass% TiO$_2$ addition, but comparatively less effective in further modifying the fraction of NBO/Si species within the molten slag structure at 10 mass% TiO$_2$. This corresponds well with the observed viscosity changes observed in Figure 3 and 4.

### 3.4. Temperature Dependence and Activation Energy

**Figure 10** shows the temperature dependence of the viscosity for the CaO–SiO$_2$–17 mass% Al$_2$O$_3$–10 mass% MgO–TiO$_2$ system at CaO/SiO$_2$ of 1.2, respectively. The viscosity decreases with increasing temperatures and using the Arrhenius type relationship the apparent activation energies for viscous flow in the various slag compositions were calculated to be between 226 and 262 kJ mol$^{-1}$.[24]

### 4. Conclusion

In this study, the effect of TiO$_2$ on the viscosity in the fully liquid region of the CaO–SiO$_2$–17 mass% Al$_2$O$_3$–10 mass% MgO–TiO$_2$ slag system at various CaO/SiO$_2$ ratios was directly correlated with the slag structure revealed by FTIR and Raman.

TiO$_2$ additions lowered the viscosity by affecting the silicate network structure, where the complex silicate sheets were depolymerized into simpler silicate structures,

**Figure 9.** Fraction of [SiO$_4$]-tetrahedra stretching for various NBO/Si (1,2,3,4) species and Ti–O–Ti stretching at constant CaO/SiO$_2$ of a) 0.8 and b) 1.2.

but the aluminate structures seems to be relatively unaffected by $TiO_2$ additions. Both the Raman and FTIR analysis clearly indicate the depolymerization of the slag and closely correlates to the measured viscosity values with $TiO_2$ content. In addition, an increase in the $CaO/SiO_2$ ratio seems to be more effective in decreasing the viscosity compared to $TiO_2$ additions. From the temperature dependence at $CaO/SiO_2$ of 1.2, the activation energy of viscous flow was calculated between 226 and 260 kJ mol$^{-1}$ depending on the slag composition.

## References

[1] T. Paananen, K. Kinnunen, *Steel Res. Int.* **2009**, *80*, 408.

[2] M. V. C. Sastri, R. P. Viswanath, B. Viswanathan, *Int. J. Hydrogen Energy* **1982**, *7*, 951.

[3] G. Li, J. Ma, H. Ni, Q. Shen, F. Tsukihashi, *ISIJ Int.* **2006**, *46*, 981.

[4] T. Nagasaka, M. Hino, S. Ban-ya, *Met. Trans. B* **2000**, *31B*, 945.

[5] A. Shankar, M. Görnerup, A. K. Lahiri, S. Seetharaman, *Met. Trans. B* **2006**, *37B*, 941.

[6] L. B. McRae, E. Pothast, P. R. Jochenst, D. D. Howat, *J. SAIMM* **1969**, *69*, 577.

[7] K. Nomura, B. Ozturk, R. J. Fruehan, *Met. Trans. B* **1991**, *37B*, 783.

[8] J. Tanabe, H. Suito, *Steel Res. Int.* **1992**, *63*, 515.

[9] Y. Morizane, B. Ozturk, R. J. Fruehan, *Met. Trans. B* **1999**, *30B*, 29.

[10] M. Chapman, O. Ostrovski, G. Tranell, S. Jahanshahi, *Elektrometallurgiya* **2000**, *3*, 34.

[11] M. Kato, S. Minowa, *Trans. Iron Steel Inst. Jpn.* **1969**, *9*, 31.

[12] G. Handfield, G. G. Charette, *Can. Metall. Q* **1971**, *10*, 235.

[13] A. Ohno, H. U. Ross, *Can. Metall. Q* **1963**, *2*, 259.

[14] N. Saito, N. Hori, K. Nakashima, K. Mori, *Met. Trans. B* **2003**, *34B*, 509.

[15] K. Datta, P. K. Sen, S. S. Gupta, A. Chatterjee, *Steel Res. Int.* **1993**, *64*, 232.

[16] R. Yamamoto, R. Nakajima, Y. Koyama, K. Niiya, *Ironmaking Conf. Proc, ISS-AIME, Detroit, MI*, **1985**, *44*, p. 149.

[17] M. Higuchi, *Trans. ISS, I&S* **1978**, 33.

[18] L. Zhang, L. Zhang, M. Wang, G. Li, Z. Sui, *ISIJ Int.* **2006**, *46*, 458.

[19] A. Shankar, M. Görnerup, A. K. Lahiri, S. Seetharaman, *Met. Trans. B* **2007**, *38B*, 911.

[20] H. Kim, W. H. Kim, I. Sohn, D. J. Min, *Steel Res. Int.* **2010**, *81*, 261.

[21] H. Kim, I. Sohn, *ISIJ Int.* **2011**, *51*, 1.

[22] S. Sridhar, K. C. Mills, O. D. C. Afrange, H. P. Lorz, R. Carli, *Ironmaking Steelmaking* **2000**, *27*, 238.

[23] W. Wang, A. Cramb, *Steel Res. Int.* **2008**, *79*, 271.

[24] I. Sohn, W. Wang, H. Matsuura, F. Tsukihashi, D. J. Min, *ISIJ Int.* **2012**, *52*, 165.

[25] V. Mikailov, E. Belyakova, *Ural Met.* **1939**, *6*, 7.

[26] S. Banya, *122–123rd Nishiyama Memorial Lecture Series*, Iron and Steel Institute of Japan, Tokyo **1988**, p. 4.

[27] R. G. Ward, *An Introduction to the Physical Chemistry of Iron and Steelmaking*, Edward Arnold, London **1972**, p. 120.

[28] S. M. Han, J. G. Park, I. Sohn, *J. Non-Cryst. Solids* **2010**, *357*, 2868.

[29] S. Agathopoulos, D. U. Tulyaganov, J. M. G. Ventura, S. Kannan, A. Saranti, M. A. Karakassides, J. M. F. Ferreira, *J. Non-Cryst. Solids* **2006**, *352*, 322.

[30] B. O. Mysen, D. Virgo, C. M. Scarfe, *Am. Miner.* **1980**, *65*, 690.

[31] Y. Tsunawaki, N. Iwamoto, T. Hattori, A. Mitsuishi, *J. Non-Cryst. Solids* **1981**, *44*, 369.

[32] Y. Iguchi, K. Yonezawa, Y. Funaoka, S. Banya, Y. Nishina, Proc. 3rd Int. Conf. Molten Slags and Fluxes, Glassgow, **1989**, p. 169.

[33] B. O. Mysen, F. J. Ryerson, D. Virgo, *Am. Miner.* **1980**, *65*, 1150.